

High-Throughput Screen for Novel Antimicrobials using a Whole Animal Infection Model

Terence I. Moy^{†,*§}, Annie L. Conery^{*§}, Jonah Larkins-Ford^{*§}, Gang Wu^{*§}, Ralph Mazitschek[¶], Gabriele Casadei[‡], Kim Lewis[‡], Anne E. Carpenter^{||}, and Frederick M. Ausubel^{†,*§,*}

[†]Department of Genetics, Harvard Medical School, Boston, Massachusetts 02115, [‡]Department of Molecular Biology, [§]Center for Computational and Integrative Biology, and [¶]Center for Systems Biology, Massachusetts General Hospital, Boston, Massachusetts 02114, [‡]Department of Biology, Northeastern University, Boston, Massachusetts 02115, and ^{||}Imaging Platform, Broad Institute of MIT and Harvard, Cambridge, Massachusetts 02142

Identifying new classes of antimicrobial drugs is imperative due to the growing threat of antibiotic-resistant bacteria in both nosocomial and community settings. Traditionally, new antibiotics are discovered using assays that measure growth inhibition or killing of a microbial pathogen (1), but the rate of new antibiotic discovery using this approach has been disappointingly slow (1–5). This is partly because traditional *in vitro* and whole cell drug screens are inefficient, yielding compounds that are non-specifically toxic or compounds with the same mechanism of action as known antibiotics. Antibiotics currently in use inhibit about 40 bacterial targets, all of which affect the growth or survival of the bacteria (6).

Previously, we developed a unique approach to the discovery of novel antimicrobials that is based on the idea of screening for anti-infective properties of drugs in an environment that better approximates an infected human host than current *in vitro* models. This was achieved by assaying survival of a live model host organism, the nematode *Caenorhabditis elegans*, infected with the human opportunistic pathogen *Enterococcus faecalis* (7). The use of live, infected whole animals to screen for antimicrobial compounds advances the established paradigm for identifying antibiotics in several key ways. First, the whole animal approach directly assesses drug efficacy *in vivo*, discarding compounds toxic to

the host early in the analysis. Also, unlike conventional *in vitro* screens, this strategy can identify compounds that target the processes by which microbes establish infections, specifically, mechanisms that are only manifest when the complex host/pathogen relationship is intact. Furthermore, because possible targets such as those related to pathogen virulence or host immunity are not likely to be essential genes, they may not be subject to a high level of selection pressure in the environment and may not be as susceptible to the development of drug resistance as essential targets.

Previously, we completed a small-scale, manual screen of 6,000 compounds and 1,136 natural product extracts that identified 16 compounds and extracts that promoted nematode survival after exposure to *E. faecalis* (7). Several of these cure *C. elegans* of a bacterial infection *in vivo* but do not affect the free-living microbe, indicating that whole animal screening can identify compounds with novel targets. Although successful, our small-scale *C. elegans* screen involved many tedious manual manipulations that introduced variability and represented hours of labor, including many spent screening individual nematodes by eye at a microscope. Here, we describe the development of an automated *C. elegans* screening system that decreases manual labor and experimental variability, thereby increasing the throughput of screening and

ABSTRACT The nematode *Caenorhabditis elegans* is a unique whole animal model system for identifying small molecules with *in vivo* anti-infective properties. *C. elegans* can be infected with a broad range of human pathogens, including *Enterococcus faecalis*, an important human nosocomial pathogen. Here, we describe an automated, high-throughput screen of 37,200 compounds and natural product extracts for those that enhance survival of *C. elegans* infected with *E. faecalis*. Using a robot to dispense live, infected animals into 384-well plates and automated microscopy and image analysis, we identified 28 compounds and extracts not previously reported to have antimicrobial properties, including six structural classes that cure infected *C. elegans* animals but do not affect the growth of the pathogen *in vitro*, thus acting by a mechanism of action distinct from antibiotics currently in clinical use.

*Corresponding author, ausubel@molbio.mgh.harvard.edu.

Received for review April 7, 2009 and accepted June 8, 2009.

Published online June 29, 2009
10.1021/cb900084v CCC: \$40.75

© 2009 American Chemical Society

accuracy of the data. We accomplished this through miniaturization to a 384-well plate format compatible with high-throughput chemical screens, the use of a large particle sorter to dispense living worms into the wells, imaging of wells with automated microscopy, and the development of software to quantify worm survival from the images. Using these methods, we screened approximately 37,000 small molecules and natural product extracts for those that increased survival of *C. elegans* infected with *E. faecalis*. We identified 28 compounds that have confirmed curing activity but which were not known antibiotics, structural analogues of antibiotics, or compounds with documented antimicrobial activity. Of these 28 compounds, 6 are of high interest because they inhibit pathogen growth *in vivo* in a live host but do not significantly inhibit microbial growth *in vitro*, suggesting that they may be functioning as virulence inhibitors or host immune enhancers in the *C. elegans* model and thus are distinct from traditional antibiotics. In addition, with the automation of a *C. elegans* screen for anti-infectives, we have developed a scalable and adaptable system that can be applied to a broad range of whole animal screens.

High-Throughput Assay Development.

Our goal was to identify anti-infective compounds through a quantitative, high-throughput *C. elegans* screen, based on our previous, small-scale assay (7). To improve the screening rate and accuracy, we automated several steps (Figure 1, panel a). First, we used a large particle sorter to dispense an exact number of infected animals into each well of a 384-well compound plate. Because human screening of the plates is too slow, labor-intensive, and subjective for high-throughput screening, we developed a staining method to distinguish live from dead worms. We stained the worms with SYTOX Orange, which is excluded by living cells but readily enters cells with damaged membranes, specifically staining dead worms (8). Because the

SYTOX dye also stains the bacteria in the well, we added a wash step to remove the bacteria before staining. Next, we used an automated microscope to acquire an image of the SYTOX fluorescence and a bright field image of each well. We then quantified worm survival in an automated manner by adapting the open-source cell image analysis program CellProfiler (9). We also created a web-based interface for viewing the original images and CellProfiler outputs, as well as to perform additional analyses (Supplementary Figure 1). The availability of the original images and the deposition of our data into the publicly available ChemBank database (10) provide a powerful resource for future data mining.

To create an automated image analysis system robust enough for high-throughput screening, we developed a complex CellProfiler pipeline consisting of 29 steps to analyze images. The major steps of this pipeline are shown in Figure 1, panel b (see also Supplementary Method 1). The general approach was to measure the area of each well that was SYTOX-positive in the fluorescence image and normalize by the total area occupied by all worms, as quantified in the bright field image. This required illumination correction to flatten lighting abnormalities, adaptive thresholding, and size- and contrast-based filters and masks to exclude debris and other artifacts. By calculating the ratio of fluorescent area to total area, we were able to accurately quantify worm death in each well. As shown in Figure 1, panel b, when 12 of the 14 worms are dead in a well as scored manually by shape (live worms are sinusoidal, whereas dead worms are rigid rods), the ratio of fluorescent area to total worm area is 0.78. In a well where the worms are rescued by ampicillin treatment, 3 of the 14 worms are dead and the ratio obtained by CellProfiler analysis is correspondingly low at 0.12.

The SYTOX analysis method was sufficiently accurate for automated, high-throughput screening (Figure 2, panel a). In

an assay with duplicate 384-well plates where half of the wells contained 21 $\mu\text{g mL}^{-1}$ ampicillin and the other half contained DMSO as a mock treatment, there was no overlap in scores between the mock (range = 0 to 0.3) and antibiotic (range = 0.85 to 0.95) treatment. The Z' -factor for the assay was 0.61, which denotes that the mean scores of the control populations are separated by several standard deviations and that the screening method is extremely robust (11).

We also compared the accuracy of the automated image analysis method to manual, body-shape-based scoring. Scoring the same set of control images with the two methods, we found that in general worm survival determined by the automated method correlates well with the manual method in a simple regression line with the $R^2 = 0.98$ (Figure 2, panel b). We observed a small fraction of worms that appeared dead on the basis of their body shape but did not stain with SYTOX (one example is seen in the ampicillin-treated well in Figure 1, panel b) and another small fraction of sinusoidal worms that were SYTOX-stained. These discrepancies may be due to variability in SYTOX staining, autofluorescence that occurs in sick or dying worms, or SYTOX staining of dying cells in worms that are still alive. In the case of SYTOX staining of live worms, an interesting possibility is that particular compounds may increase the membrane permeability of the worms to the dye. To make the automated analysis directly comparable to the more conventional shape-based scoring method would require algorithms to identify and measure the shape of individual worms. We have begun to develop such algorithms, which would also enable screens for a wide array of phenotypes, such as changes in morphology or fluorescence localization.

Currently, a set of 30 384-well plates requires 8 h of worm dispensing. The same set of 30 plates also requires a full day to image and another day for image analysis.

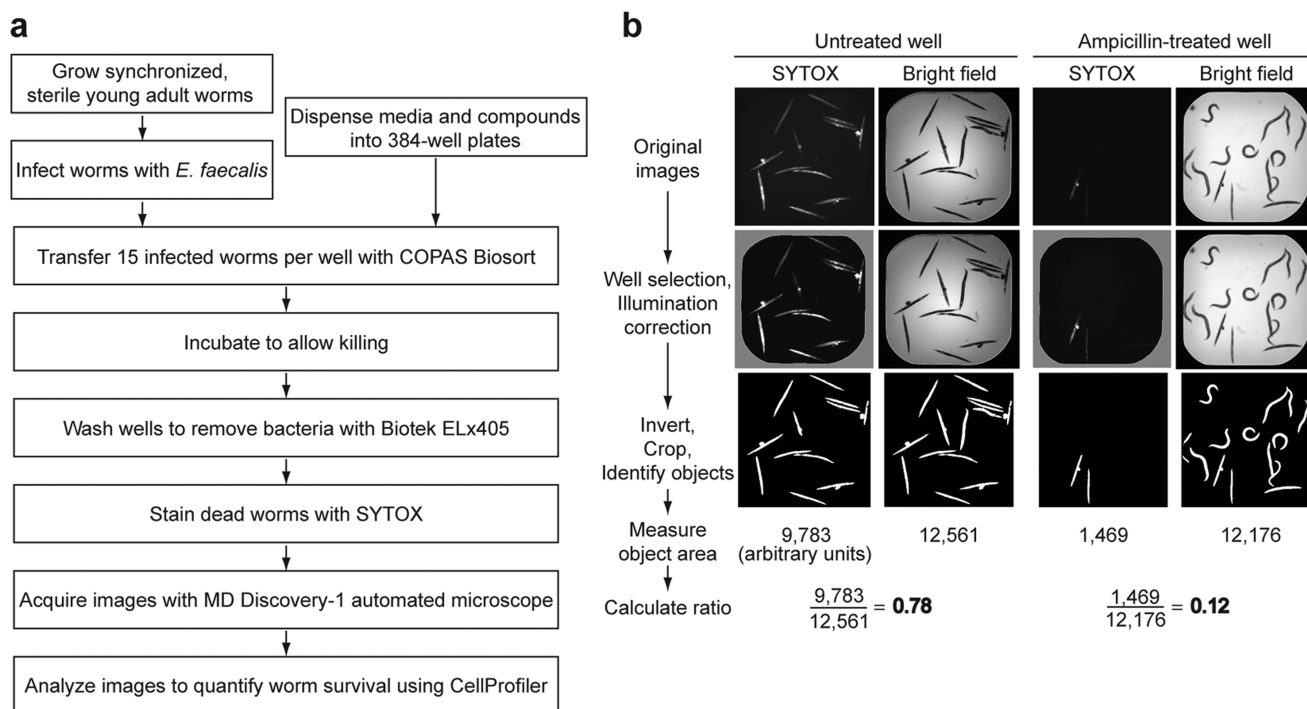


Figure 1. Automated, high-throughput *C. elegans* infection screen. a) Screening scheme. b) Major steps of CellProfiler image analysis. The original SYTOX fluorescence and bright field images of untreated and ampicillin-treated wells, as well as images after CellProfiler manipulations, and data from the analysis are shown.

Scoring the plates using the automated SYTOX live/dead assay is ~ 5 times faster than scoring the plates manually. Thus, this versatile and robust automated whole animal screening system accommodates $\sim 9,000$ compounds per week, per researcher, thereby enabling screens that were previously not feasible due to the amount of labor and time required for manual scoring.

Although there have been examples of manual and semiautomated small molecule screens with *C. elegans* and other model organisms (12–14), our system is unique in its adaptability and scalability. All instrumentation is commercially available, and the software is open-source (www.CellProfiler.org). The methodology is immediately applicable to *C. elegans* screens with a live or dead readout, including screens to identify compounds that have anti-infective

activity against other pathogens, that extend lifespan, or that kill pathogenic nematodes. The approach can also be easily adapted for a broad range of small molecule screens using whole animals to probe a variety of biological processes, for example, to identify modifiers of gene expression or behavior that are linked to changes in fluorescence.

High-Throughput Screen. Using these methods, we screened approximately 54,000 wells in duplicate from multiple compound collections, including known bioactives, natural product extracts, purified natural products, or synthetic compounds (Table 1). Because several of the compound collections contained identical compounds, we screened 33,931 unique compounds and 3,283 natural product extracts. For each of the 17 independent batches of plates, we included two 384-well plates that con-

tained only the mock treatment. This enabled the Broad Chemical Biology Platform to generate a z-score value for each sample, which represents the number of standard deviations the sample well ratio is apart from the ratio of the mock-treated wells (10). Each screening assay also included duplicate positive and negative control plates in which half of the wells contained ampicillin or DMSO (mock) treatment. A mock-treated well should have a z-score of 0, and a well with increased worm survival should have a negative z-score because it has a lower ratio of dead to total area. The screen average for mock-treated wells was -0.14 with a standard deviation of 0.71. For ampicillin-treated wells, the average was -8.70 with a standard deviation of 0.61.

In the primary screen, a composite z-score was calculated from the two replicates for each compound. The composite

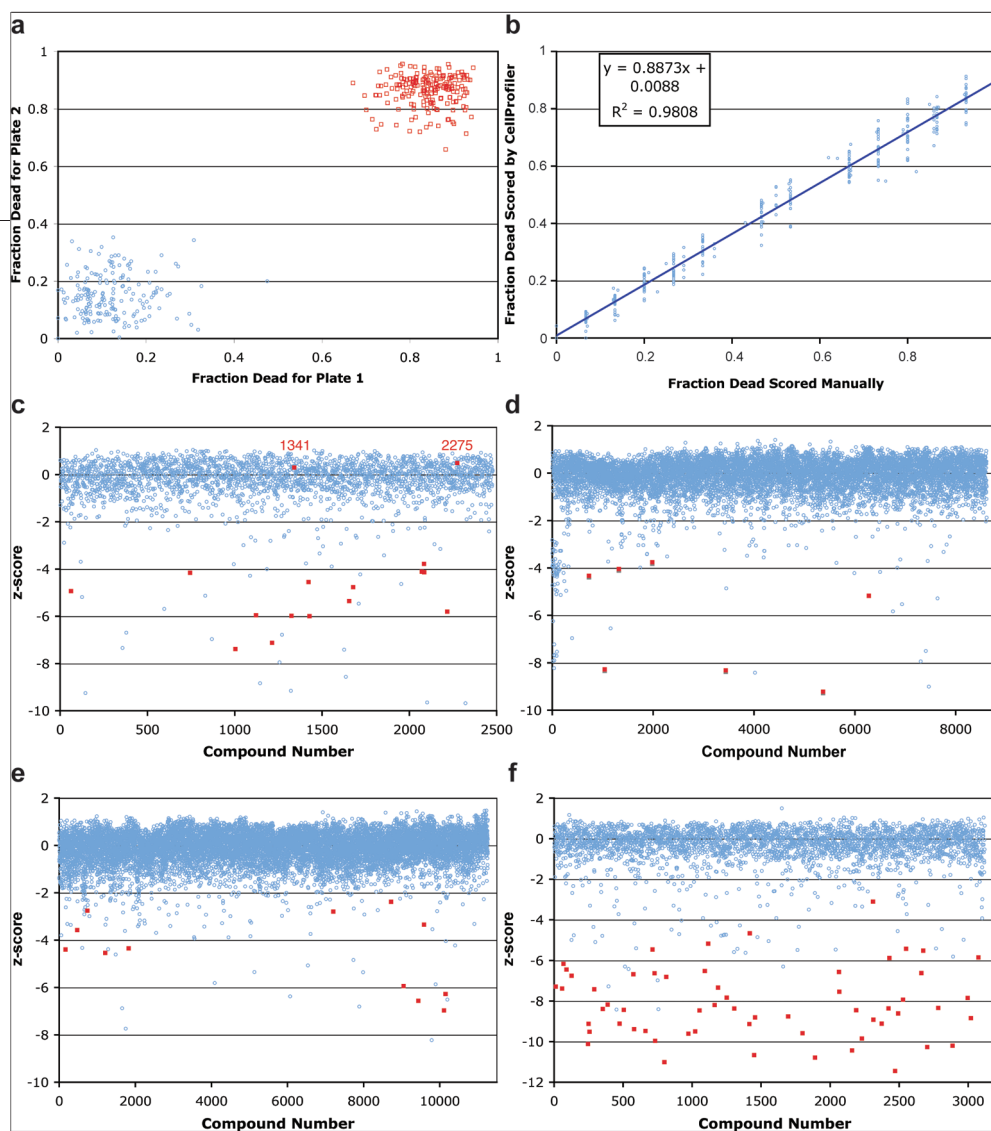


Figure 2. Robust screening methods. a) A large separation is seen between the fraction dead of ampicillin and mock-treated control wells from two control plates. Red squares are values for mock-treated control wells, and the blue circles are for ampicillin-treated control wells. b) Linear regression plot correlating manually scored data with CellProfiler scored data. Worm survival determined by the automated method correlates well with the manual method in a simple regression line with the $R^2 = 0.98$. c–f) z-score values for compounds in four libraries (panel c, Analyticon; panel d, TimTec, panel e, ChemDiv; and panel f, SPBio). Blue circles represent z-scores of compounds, and the positive hits from manual scoring are highlighted as red squares. The false negative compounds that were hits by manual screening but had z-scores near 0 are labeled as red numbers.

z-scores were sorted in ascending order and approximately the top 1% of the compounds was selected for confirmation by manual analysis of the original images based on body shape, a reasonable number to score by eye. “False-positive” wells excluded from further analysis included cases with low fluorescence signal with straight body position, debris, or compound precipitation that was quantified as total worm area, the absence of worms in the well due to inaccurate worm sorting, poor image quality due to well abnormalities, or cases

where only one of the two duplicate wells showed increased survival.

To determine the false negative rate of the automated analysis method, we manually screened a random set of 4,954 bright-field images for one of the library collections. We identified 16 wells that showed increased survival for both duplicate wells (Figure 2, panel c). Fourteen of these wells were also identified by the automated analysis method. The two wells that were not identified by the automated analysis, corresponding to compounds 1341 and 2275, were

missed because the worms with sinusoidal, live body position were SYTOX-positive with corresponding z-scores of 0.3 and 0.5. A similar number of bright-field images for other compound libraries were also screened and no more false negatives were identified, suggesting that they occur at a very low frequency (Figure 2, panels d–f).

Analysis of Novel Identified

Anti-infectives. The screen identified 132 compounds and 4 extracts that increased worm survival, with an overall hit rate of approximately 0.25% (Table 1 and Supplementary Figure 2). Among the 136 primary hits, we identified 16 pairs of duplicate compounds from different compound libraries, indicating that the assay is consistent between experiments. However, we also found 5 hit compounds among the 136 primary hits that had duplicates in other libraries that were not identified as hits. In general, these latter 5 hits had relatively weak activity. Of the primary hits, 119 compounds and extracts were available for cherry picking

and retesting in a secondary screen, and 108 of the 119 compounds and extracts (91%) retested as positive in a second experiment. Of these, 62 are known antibiotics and 18 others have reported antimicrobial properties or are structural analogues of known antibiotics. These 80 known or suspected antibiotics include 15 of the 16 pairs of duplicate compounds. Of the remaining 27 unique hits, we were able to purchase 21 compounds for further testing.

We determined the minimum inhibitory concentrations (MIC) of the 21 commer-

TABLE 1. Compound libraries screened and the number of members from each library identified as having curing activity in *C. elegans* infected with *E. faecalis*

Compound library	Wells screened	Hits	Hit rate (%)
Bioactives	2,000 ^a	69	3.50 ^a
Natural product extracts	3,283	4	0.12
Analyticon purified natural products	2,477	18	0.65
Diversity-oriented synthesis (DOS)	11,666	1	0.01
ChemBridge kinases	8,240	21	0.27
Commercial compounds:			
ChemDiv	11,616	12	0.10
TimTec	8,512	7	0.08
MayBridge	5,448	3	0.06
ChemBridge	704	1	0.14
Total	53,946 ^b	136	0.24 ^c

^aApproximate number due to redundancies. ^b33,931 unique compounds and 3,283 extracts.

^cAverage hit rate.

cially available compounds *in vitro* with *E. faecalis* and performed dose response time course experiments to determine the kinetics of their activity in the infection assay (Table 2 and Supplementary Figures 3, 4). We found that 9 of the 21 compounds cure *C. elegans* of an *E. faecalis* infection at a significantly lower concentration than is necessary to inhibit the growth of the pathogen *in vitro*, the hallmark of an anti-infective compound that targets pathogen virulence or host immunity. Four of the 9 compounds share a structural backbone (structural group 1 of Table 2 and Supplementary Figure 4), and 3 of the remaining 5 anti-infective compounds (groups 2–4 of Table 2 and Supplementary Figure 4) each had another compound with a shared backbone that was identified as having curing activity. Supplementary Figure 3 shows dose response curves illustrating the curing kinetics for a representative compound from each of the 6 anti-infective structural classes. One other compound (structural group 7 of Supplementary Figure 4) also exhibited anti-infective properties but, because the curing

activity was weak, was not included in subsequent studies.

Interestingly, 8 compounds, representing 2 structural classes (groups 1 and 2 of Table 2 and Supplementary Figure 4), are similar to two structural groups that were identified previously in a screen for inhibitors of *Pseudomonas aeruginosa* biofilm development (15). Also, another structural group (group 3 in Table 2 and Supplementary Figure 4) was identified in a screen for O-GlcNAc transferase inhibitors (16). The activity of these small molecules in other screens suggests a mechanism by which the compounds promote worm survival in our assay. Intriguingly, inhibition of biofilm formation and eradication of established biofilms have been postulated to be mechanisms for antivirulence factors (17, 18), and the discovery of biofilm inhibitors in our screen suggests that such factors may be able to cure infections in an *in vivo* setting. Furthermore, biofilm blockers may dramatically change clinical treatment regimens since persistent pathogen infections normally present in biofilms are extremely difficult to eradicate with conventional antibiot-

ics (17, 18). Importantly, we have also identified 3 novel classes of compounds (groups 4, 5, and 6 in Table 2 and Supplementary Figure 4) that may represent small molecules with novel targets in pathogenesis and immunity.

Our high content screen of ~37,000 compounds identified 6 structural classes of compounds that we classify as anti-infectives rather than traditional antibiotics because they cure infected *C. elegans* animals without affecting the growth of the pathogen *in vitro*. The screen also identified many known antibiotics, antimicrobials, and compounds with known antivirulence activity, which serves as a proof of principle for the screen. Furthermore, the identification of three novel structural classes of compounds validates that high-throughput, whole organism *C. elegans* screening will reveal compounds acting through novel mechanisms of action. In addition, the whole animal screening system we developed makes possible the direct study of complex biological processes such as growth, reproduction, aging, and immunity, which would not be possible *in vitro* or with a cell-based system. Despite the challenges, our discoveries indicate that screening in a living animal confers strong advantages, with profound implications for drug discovery efforts as well as for basic biological research. We are using the novel small molecules identified in the screen to probe bacterial pathogenesis and *C. elegans* innate immunity, while also identifying the targets of these compounds and investigating their clinical relevance.

METHODS

Infection Assay for Primary Compound Screen.

glp-4(bn2);sek-1(km4) mutant worms were grown to gravid adult stage (19, 20). One thousand worms at the L1 stage were grown for 5.2 days at 15 °C on 9 cm plates of SK agar media (21) spread with a lawn of *E. coli* strain HB101. Embryos from the gravid adults were isolated by a previously described hypochlorite method (22) and hatched at 15 °C for 2 days; 4,500 of the L1 hatchlings were grown on each 9 cm plate of SK-NS agar (SK media with 62.5 U mL⁻¹ nystatin and 100 µg mL⁻¹

TABLE 2. Representative structures for the six anti-infective structural groups identified in the screen and their corresponding MIC and minimum EC values

Group	Compound Structure	MIC	EC
1		25	1.56
2		1.56	0.39
3		6.25	0.39
4		>100	25
5		>100	3.13
6		>100	3.13

streptomycin) and with lawns of *E. coli* HB101. These worms were grown at 25 °C for 52 h to generate sterile, young adults. A culture of *E. faecalis* MMH594 was grown in BHI broth (BD Difco) with 80 $\mu\text{g mL}^{-1}$ kanamycin at 37 °C for 6 h, and 100 μL of the culture was spread onto each 9 cm plate of BHI agar containing 80 $\mu\text{g mL}^{-1}$ kanamycin. Lawns of *E. faecalis* were grown at 25 °C for 16 h and transferred to 15 °C for 8 h.

Sterile adult worms were resuspended in M9 buffer (23) and washed two times with M9 in a 1:10 ratio to remove *E. coli*. Then, 8,000 worms

were pipetted onto each lawn of *E. faecalis* and incubated 15 h at 15 °C. After infection, the worms were resuspended in M9 and used as described below. The 384-well plates (Corning no. 3712) were filled with 55 μL of media (see below) using a Thermo Scientific Multidrop Combi reagent dispenser, and 0.3 μL of compound in DMSO was pin transferred into each well using a CyBio CyBi-Well vario transfer system. The plates were agitated using an Eppendorf MixMate at 1,800 rpm for 15 s. Using the Union Biometrica Complex Object Parametric Analyzer and Sorter (COPAS) BioSort worm

sorter according to manufacturer's protocols, 15 of the infected worms were transferred to each well in a total volume of approximately 15 μL . Total volume per well is 70 $\mu\text{L well}^{-1}$ with a final composition of the media being 20% BHI, 60% M9 buffer, 80 $\mu\text{g mL}^{-1}$ kanamycin, 62.5 U mL^{-1} nystatin, 1% DMSO, and 19% sheath solution (Union Biometrica Part no. 300-5101-000). Plates were vortexed for 5 s, centrifuged at 1000g for 10 s, and sealed with gas permeable membranes (Breath-Easy, Diversified). Plates were placed in a single layer on the top shelves in a 26.3 °C incubator at 85% relative humidity (RH) and incubated without agitation for 5 days.

After 5 days, the bacteria and liquid media in the assay plates were removed as described below. First, the bacteria were resuspended by shaking on the MixMate for 15 s at 1,800 rpm, the sealing membrane was removed, and the worms were allowed to settle to the bottom of the wells for 3 min. Using the BioTek ELx405 microplate washer with the BioStack plate handling system according to manufacturer's guidelines, approximately 70% of the liquid in the wells were aspirated. Then, 65 μL of M9 buffer was dispensed into the wells at maximum speed to resuspend the well contents. The worms were allowed to settle for at least 3 min, and then three more cycles of aspiration, dispensing, and settling were performed. Lastly, one final round of aspiration was performed leaving approximately 20 μL of liquid in the well. Then 70 μL of 0.9 μM SYTOX Orange (Invitrogen) in M9 was dispensed into each well with the Combi dispenser to yield a final concentration of 0.7 μM of dye. The plates were sealed with gas permeable membranes and incubated at 20 °C and 80% RH for 16 h. Using a Molecular Devices Discovery-1 microscope with a transmitted light module and a 2x low magnification objective running MetaExpress software, images showing the entire well were captured using a TRITC filter set or with bright field transmitted light.

The screen was performed using duplicate plates. For every experiment, one set of duplicate plates consisted entirely of mock treatment (DMSO only). Another set of duplicate plates each contained 192 wells of ampicillin at a final concentration of 21 $\mu\text{g mL}^{-1}$ as a positive control and 192 wells of mock treatment as the negative control. The primary screen was performed with 17 independent infection assays where a total of 33,931 compounds and 3,283 natural product extracts were screened at the Broad Institute's Chemical Biology Platform Screening Facility.

Data Storage and CellProfiler Analysis. All images acquired at the Broad Institute were transferred to and stored on a dedicated Dell PowerEdge 2950 server attached directly to 15 1TB SATA hard drives at Massachusetts General Hospital. Data analysis was carried out on the Dell 2950 server with CellProfiler (www.cellprofiler.org) using a customized pipeline (Supplementary Method 1), and the resulting processed images and associated data were loaded into a custom Oracle database developed specifically for this project.

Dose Response Time Courses. The infection assay was performed essentially as described above,

except SYTOX staining was not used. Instead, brightfield images of the wells were acquired at daily time points and scored manually for worm survival by analyzing worm body positioning. The effective concentrations (EC) were calculated as the concentrations at which the dose response curves of a compound (converted to Kaplan–Meier survival plots) were significantly different from the mock-treated sample with a p -value < 0.05 , according to the logrank statistical analysis. All purchased compounds used in secondary assays were confirmed for identity and purity by LC/MS (Supplementary Method 2).

Scoring Control Plates for Manual versus Automated Methods Comparison.

Synchronized young adult worms were grown on *E. coli* HB101 on SK-NS agar plates at 25 °C as described above. To generate dead worms, the worms were washed with M9 buffer and then incubated in M9 buffer at 42 °C for 2 h. The COPAS Biosort was used to transfer 15 live or dead worms into a 384-well plate containing M9 buffer and 0.7 μM SYTOX Orange. The worms were incubated for 4 h at 22 °C, fluorescence and bright field images were taken for each well, and images were scored as described.

MIC Assays. A culture of *E. faecalis* MMH594 was grown overnight in BHI broth to stationary phase at 37 °C with aeration. The culture was diluted to an approximate density of 2×10^{-4} CFU mL^{-1} in worm infection media (20% BHI, 80% M9 buffer), and 12.5 μL of the bacterial culture dilution was inoculated into 384-well plates containing 12.5 μL of 2-fold serial dilutions of the compounds. All wells had a final DMSO concentration of 1%. Plates were incubated at 37 °C for 15 h and scored by eye for bacterial growth.

Acknowledgment: We thank the Broad Institute of MIT and Harvard Chemical Biology Platform screening facility staff including L. Verplank, A. Stern, J. Burbank, S. Norton, M de Silva, K. Rose, M. Bliss-Moreau, and N. Tolliday for assistance with chemical screening and many helpful discussions. We thank T. R. Jones of the Broad Institute Imaging Platform for contributions to image analysis algorithms. This work was funded by a grant from the Broad Institute of Harvard and MIT and by National Institutes of Health grant AI072508 and in part with Federal funds from the National Cancer Institute's Initiative for Chemical Genetics, NIH, under Contract N01-CO-12400. A.E.C. was supported by a Novartis Fellowship of the Life Sciences Research Foundation. The content of this publication does not necessarily reflect the views or policies of the Department of Health and Human Service, nor does mention of trade names, commercial products, or organizations imply endorsement by the U.S. Government.

Supporting Information Available: This material is available free of charge via the Internet at <http://pubs.acs.org>.

REFERENCES

- Walsh, C. (2003) Where will new antibiotics come from? *Nat. Rev. Microbiol.* **1**, 65–70.
- Boggs, A. F., and Miller, G. H. (2004) Antibacterial drug discovery: is small pharma the solution? *Clin. Microbiol. Infect.* **10**, (4), 32–36.
- Projan, S. J., and Shlaes, D. M. (2004) Antibacterial drug discovery: is it all downhill from here? *Clin. Microbiol. Infect.* **10**, (4), 18–22.
- Schmid, M. B. (2004) Seeing is believing: the impact of structural genomics on antimicrobial drug discovery, *Nat. Rev. Microbiol.* **2**, 739–746.
- Silver, L. L. (2005) A retrospective on the failures and successes of antibacterial drug discovery, *IDrugs* **8**, 651–655.
- Bumann, D. (2008) Has nature already identified all useful antibacterial targets? *Curr. Opin. Microbiol.* **11**, 387–392.
- Moy, T. I., Ball, A. R., Anklesaria, Z., Casadei, G., Lewis, K., and Ausubel, F. M. (2006) Identification of novel antimicrobials using a live-animal infection model, *Proc. Natl. Acad. Sci. U.S.A.* **103**, 10414–10419.
- Gill, M. S., Olsen, A., Sampayo, J. N., and Lithgow, G. J. (2003) An automated high-throughput assay for survival of the nematode *Caenorhabditis elegans*, *Free Radical Biol. Med.* **35**, 558–565.
- Carpenter, A. E., Jones, T. R., Lamprecht, M. R., Clarke, C., Kang, I. H., Friman, O., Guertin, D. A., Chang, J. H., Lindquist, R. A., Moffat, J., Golland, P., and Sabatini, D. M. (2006) CellProfiler: image analysis software for identifying and quantifying cell phenotypes, *Genome Biol.* **7**, R100.
- Seiler, K. P., George, G. A., Happ, M. P., Bodycombe, N. E., Carrinski, H. A., Norton, S., Brudsz, S., Sullivan, J. P., Muhlich, J., Serrano, M., Ferraiolo, P., Tolliday, N. J., Schreiber, S. L., and Clemons, P. A. (2008) ChemBank: a small-molecule screening and cheminformatics resource database, *Nucleic Acids Res.* **36**, D351–359.
- Zhang, J. (1999) A simple statistical parameter for use in evaluation and validation of high throughput screening assays, *J. Biomol. Screening* **4**, 67–73.
- Kwok, T. C., Ricker, N., Fraser, R., Chan, A. W., Burns, A., Stanley, E. F., McCourt, P., Cutler, S. R., and Roy, P. J. (2006) A small-molecule screen in *C. elegans* yields a new calcium channel antagonist, *Nature* **441**, 91–95.
- Petrasccheck, M., Ye, X., and Buck, L. (2007) An antidepressant that extends lifespan in adult *Caenorhabditis elegans*, *Nature* **450**, 553–556.
- Tran, T. C., Sneed, B., Haider, J., Blavo, D., White, A., Aiyerjorun, T., Baranowski, T. C., Rubinstein, A. L., Doan, T. N., Dingleline, R., and Sandberg, E. M. (2007) Automated, quantitative screening assay for antiangiogenic compounds using transgenic zebrafish, *Cancer Res.* **67**, 11386–11392.
- Junker, L. M., and Clardy, J. (2007) High-throughput screens for small-molecule inhibitors of *Pseudomonas aeruginosa* biofilm development, *Antimicrob. Agents Chemother.* **51**, 3582–3590.
- Gross, B. J., Kraybill, B. C., and Walker, S. (2005) Discovery of O-GlcNAc transferase inhibitors, *J. Am. Chem. Soc.* **127**, 14588–14589.
- Marra, A. (2006) Targeting virulence for antibacterial chemotherapy: identifying and characterising virulence factors for lead discovery, *Drugs R&D* **7**, 1–16.
- Cegelski, L., Marshall, G. R., Eldridge, G. R., and Hultgren, S. J. (2008) The biology and future prospects of antivirulence therapies, *Nat. Rev. Microbiol.* **6**, 17–27.
- Tanaka-Hino, M., Sagasti, A., Hisamoto, N., Kawasaki, M., Nakano, S., Ninomiya-Tsuji, J., Bargmann, C. I., and Matsumoto, K. (2002) SEK-1 MAPKK mediates Ca^{2+} signaling to determine neuronal asymmetric development in *Caenorhabditis elegans*, *EMBO Rep.* **3**, 56–62.
- Beanan, M. J., and Strome, S. (1992) Characterization of a germ-line proliferation mutation in *C. elegans*, *Development* **116**, 755–766.
- Tan, M. W., Mahajan-Miklos, S., and Ausubel, F. M. (1999) Killing of *Caenorhabditis elegans* by *Pseudomonas aeruginosa* used to model mammalian bacterial pathogenesis, *Proc. Natl. Acad. Sci. U.S.A.* **96**, 715–720.
- Powell, J. R., and Ausubel, F. M. (2008) Models of *Caenorhabditis elegans* infection by bacterial and fungal pathogens, *Methods Mol. Biol.* **415**, 403–427.
- Stiernagle, T. (2006) Maintenance of *C. elegans*, *WormBook*, and The *C. elegans* Research Community, http://www.wormbook.org/chapters/www_strainmaintain/strainmaintain.html.